J Therm Anal Calorim (2011) 105:421–426
DOI 10.1007/s10973-010-1118-9

Kinetic parameters for thermal decomposition of microcrystalline, vegetal, and bacterial cellulose

Hernani S. Barud · Clóvis A. Ribeiro · Jorge M. V. Capela · Marisa S. Crespi · Sidney. J. L. Ribeiro · Younes Messadeq

ESTAC2010 Conference Special Issue

Abstract Cellulose can be obtained from innumerable sources such as cotton, trees, sugar cane bagasse, wood, bacteria, and others. The bacterial cellulose (BC) produced by the Gram-negative acetic-acid bacterium *Acetobacter xylinum* has several unique properties. This BC is produced as highly hydrated membranes free of lignin and hemicelluloses and has a higher molecular weight and higher crystallinity. Here, the thermal behavior of BC, was compared with those of microcrystalline (MMC) and vegetal cellulose (VC). The kinetic parameters for the thermal decomposition step of the celluloses were determined by the Capela-Ribeiro non-linear isoconversional method. From data for the TG curves in nitrogen atmosphere and at heating rates of 5, 10, and 20 °C/min, the E_α and B_α terms could be determined and consequently the pre-exponential factor A_α as well as the kinetic model $g(\alpha)$. The pyrolysis of celluloses followed kinetic model $g(\alpha) = [-\ln(1-\alpha)]^{1/1.63}$ on average, characteristic for Avrami–Erofeev with only small differences in activation energy. The fractional value of n may be related to diffusion-controlled growth, or may arise from the distributions of sizes or shapes of the reactant particles.

Keywords Bacterial cellulose · Non-isothermal kinetic · Thermal decomposition

H. S. Barud · C. A. Ribeiro (✉) · J. M. V. Capela · M. S. Crespi · Sidney. J. L. Ribeiro · Y. Messadeq
Institute of Chemistry, Araraquara-Paulista State University, Av. Prof. Francisco Degni, s/n, 14800-900 Araraquara, São Paulo, Brazil
e-mail: ribeiroc@iq.unesp.br

Introduction

Cellulose is the most abundant natural biopolymer on earth, synthesized by plants and also by some species of bacteria. The ''not so green'' implications involved in cellulose extraction from plants and trees can be overcome by using bacterial cellulose (BC) [1–3].

The term "cellulose", first used by Anselme Payen in 1938, refers to a linear homopolysaccharide with a structure constituted by units of β-D-glucopyranose (β-glucose) joined by glycosidic-type β-(1 → 4), Fig. 1 [4, 5].

The linear polymer of cellulose is strongly associated through hydrogen bonds that are responsible for the formation of cellulose fibers. Cellulose molecules form intramolecular hydrogen bonds between hydroxyl groups of the same molecule and intermolecular bonds between hydroxyl groups of adjacent chains. The former type of interaction is responsible for the rigidity of the chain, and the latter for the formation of vegetable fiber.

Several chains of cellulose are arranged to form cellulose microfibrils, with regions that are disordered (amorphous regions) or highly ordered (crystalline regions). Microfibrils have a diameter of 20–30 nm and lengths that can reach several micrometers, depending on the source of cellulose (from plants, enzymatic synthesis, chemical synthesis, and some microorganisms) [6–9].

Gluconacetobacter xylinus bacteria produce cellulose that is markedly different from plant cellulose. From the culture medium, a pure-cellulose network free of lignin and hemicellulose is obtained as highly hydrated pellicles, composed of a random assembly of ribbon-shaped fibers less than 100 nm wide, denominated "nanocelluloses" [8]. The resulting supramolecular structure of hydrated BC has great mechanical strength and a large surface area formed by porous structures, which are an attractive template for

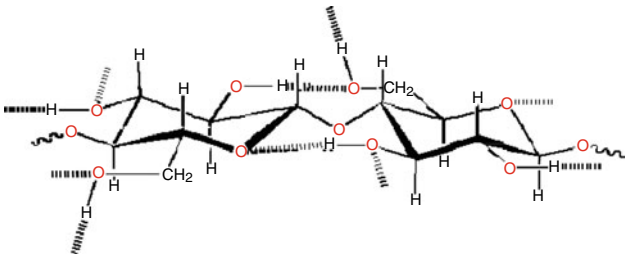

Fig. 1 Linear structure of cellulose. *The dotted lines* indicate the possible hydrogen bonds

inorganic particle stabilization [10, 11]. BC is also being used in the preparation of "green" polysaccharides composites [12], thermoplastic biofibers [13], and different types of synthetic polymers by a cross-linking reaction with organic monomers [14].

The current commercially available forms of microcrystalline cellulose (MCC) are produced from a high grade of pulps. This is hydrolyzed to "level-off degree of polymerization" (LODP) of about 200–300 and has a crystallinity of at least 78% as measured by X-ray diffraction. Since cellulose obtained from different sources differs in several properties (crystallinity, moisture, surface and pore structure, and molecular weight), different thermal behaviors are expected.

Thermal behavior

The degradation of cellulose in nitrogen has been analyzed as a first-order model having an activation energy range from 100 to 260 kJ/mol [15–18] and 100 to 160 when in air [19, 20], zero order [21], and phase boundary model [22].

Recently, the isothermal and non-isothermal kinetics for degradation of cellulose (CDH) were obtained through model-fitting (Friedman and Coats-Redfern methods) and a model-free model (Kissinger and Flynn–Wall–Ozawa methods) [23]. The F_1-type mechanism was suggested for degradation in helium atmosphere, and has an activation energy in the range of 156.5–166.5 kJ/mol and ln A of 20–23 min^{-1}.

For further evaluation of the properties of the bacterial cellulose, its thermal behavior was compared with those of microcrystalline and vegetal cellulose.

TG curves were obtained at several heating rates in nitrogen atmosphere, in order to provide the kinetic parameters by the Capela-Ribeiro iso-conversional non-isothermal method.

Kinetic parameters—non-linear isoconversional method

The kinetic parameters for the thermal decomposition step of the compound were estimated by the Capela-Ribeiro non-linear isoconversional method, using 4th-order rotational approximation of the temperature integral [24]. For a given conversion α and a set of n experiments carried out at different heating rates β_i $(i = 1\ldots.\ n)$, the parameters activation energy, E, and the B term could be determined from Eq. 1 for the least sum of squares for the plot of heating rate β for each α as a function of $z_i = 10^3/RT_i$, $(i = 1\ldots.n)$:

$$S(E \times B) = \sum_{i=1}^{n} \left(\beta_i - \frac{\exp(B - Ez_i)}{z_i} \frac{E^3 z_i^3 + 14E^2 z_i^2 + 46Ez_i + 24}{E^4 z_i^4 + 16E^3 z_i^3 + 72E^2 z_i^2 + 96Ez_i + 24} \right)^2 \quad (1)$$

$$B = \ln\left(\frac{10^3 A}{Rg(\alpha)}\right) \quad (2)$$

where A is the pre-exponential factor, R is the gas constant and $g(\alpha)$ represents the reaction mechanism.

In order to estimate the reaction model $g(\alpha)$, an expression based on both differential and integral forms of the kinetic equation can be used:

$$f(\alpha)g(\alpha) = \frac{10^3 E \mathrm{d}\alpha}{R \ \mathrm{d}T} \exp\left(\frac{10^3 E}{RT}\right) I\left(\frac{10^3 E}{RT}\right) \quad (3)$$

where $I(10^3 E/RT)$ is the integral of Arrhenius [24].

For each heating rate, the values on both sides of the Eq. 3 depend only on α. Therefore, $g(\alpha)$ could be estimated by comparing the values on the right side of the Eq. 3 against α and the theoretical master plots of $f(\alpha)g(\alpha)$ against α, Fig. 2, assuming several kinetic models from Table 1.

From the results of Eq. 3, the kinetic exponent ***n*** was estimated from the least sum of squares:

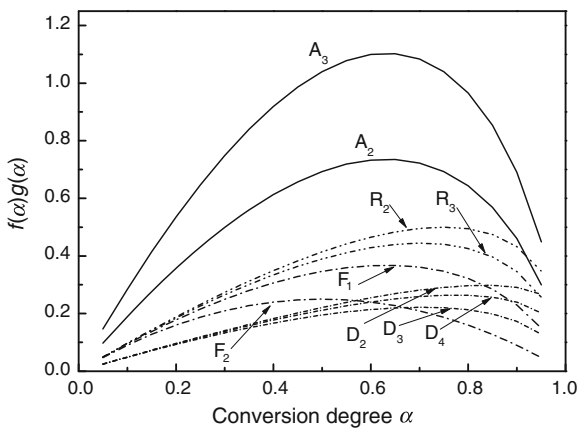

Fig. 2 Theoretical master plots of $f(\alpha)g(\alpha)$ against α for kinetic models in Table 1

Table 1 Most common expression for $f(\alpha)$ and $g(\alpha)$ functions

Symbol	Reaction model	$g(\alpha) = k(t - \tau) = kt$	$f(\alpha) = (1/k)(\mathrm{d}\alpha/\mathrm{d}t)$
R_n	Geometric models $n = 2$: Contacting area $n = 3$: Contracting volume	$1 - (1 - \alpha)^{1/n}$	$n(1 - \alpha)^{1-1/n}$
F_n or $RO(n)$	n Order		$(1 - \alpha)^n$
A_n	Avrami–Erofeev or JMAEK	$[-\ln(1 - \alpha)]^{1/n}$	$n(1 - \alpha)[-\ln(1 - \alpha)]^{1-1/n}$
D_2	Two-dimensional diffusion	$((1 - \alpha)\ln(1 - \alpha)) + \alpha$	$-\frac{1}{\ln(1 - \alpha)}$
D_3	Three-dimensional diffusion (Jander)	$(1 - (1 - \alpha)^{1/3})^2$	$\frac{3(1 - \alpha)^{2/3}}{2\left[1 - (1 - \alpha)^{1/3}\right]}$
D_4	Three-dimensional diffusion (Ginstling-Brounshtein)	$1 - \frac{2}{3}\alpha - (1 - \alpha)^{2/3}$	$\frac{3(1 - \alpha)^{1/3}}{2\left[1 - (1 - \alpha)^{1/3}\right]}$

$$\sum_{i=1}^{n}\left[f(\alpha)g(\alpha) - \frac{10^3 E\,\mathrm{d}\alpha}{R\ \ \mathrm{d}T}\exp\left(\frac{10^3 E}{RT}\right)I\left(\frac{10^3 E}{RT}\right)\right]^2 \quad (4)$$

The pre-exponential values A could be estimated by substituting the term B in Eq. 2:

$$\ln A = \ln g(\alpha) + B - \ln\left(\frac{10^3}{R}\right). \quad (5)$$

Experimental

Bacterial cellulose membranes (BC) were supplied by Fibrocel Produtos Biotecnológicos LTDA, Ibiporã, Brazil. Vegetal cellulose (VC) was obtained from mechanical and chemical (pulping) processing of wood, and commercial microcrystalline cellulose (MCC) from Avicell.

The degrees of polymerization (DP) obtained by technique of viscosity using an Ostwald viscometer according to Brazilian technical standard NBR7730 were 2800, 1300, and 225 for BC, VC, and MCC, respectively [25]. The crystallinity indexes (CrI) calculated from the DRX patterns were 76, 79, and 72% for BC, VC, and MCC, respectively [26].

Thermal behavior

Thermal degradation was followed using a TA 2960 SDT, TA Instruments in the 40–450 °C temperature range in open alumina reference and sample pans under dynamic nitrogen atmosphere (flow rate: 100 mL min^{-1}), at heating rates of 5, 10, and 20 °C min^{-1} and a sample mass around 3 mg.

Results and discussion

Figure 3 shows the TG curves for microcrystalline (MCC), bacterial (BC), and vegetal cellulose (VC) under nitrogen atmosphere and a heating rate of 10 °C/min. The first, gradual event, involving 6.9, 5.5, and 2.3% mass loss for MCC, BC, and VC, respectively, occurred from room temperature up to 230 °C, and may be associated with loss of the residual solvent. The second event, observed at around 330 °C, is attributed to cellulose pyrolysis. A residue of around 20% carbonaceous materials was observed. The thermal stability for the celluloses followed the order MCC (T_{onset} = 323.5 °C) < VC (T_{onset} = 328.6 °C) < BC (T_{onset} = 338.7 °C). MCC had a lower thermal stability than VC and BC, which was expected because of the decrease in the degree of polymerization during the hydrolysis of the MCC using diluted mineral acids [27].

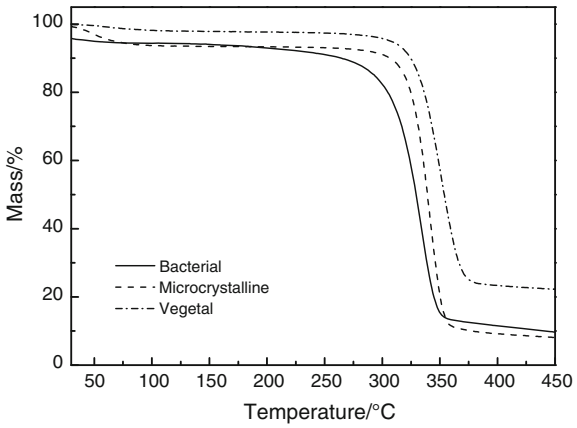

Fig. 3 TG curves for bacterial, microcrystalline, and vegetal cellulose in nitrogen atmosphere and heating rate of 10 °C/min

Figure 4 shows the set of experimental curves α–T obtained from the TG curves for BC at the heating rates of 5, 10, and 20 °C/min. The same behavior could be observed for MCC and VC. The estimative of the parameters E and B could be obtained from the least sum of squares $S(E, B)$, as defined in Eq. 1, for the plot of heating rate β_i, for each α, against z_i.

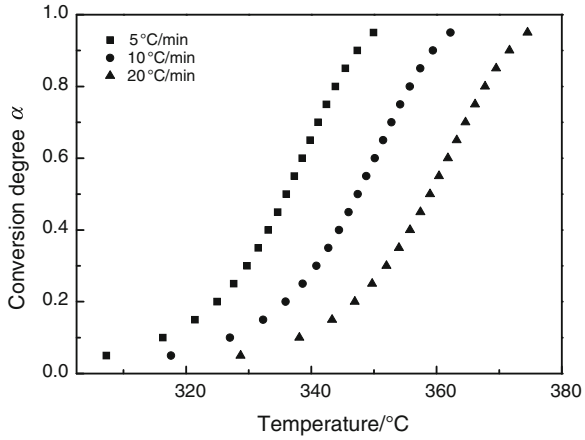

Fig. 4 Conversion degree against temperature for thermal decomposition of bacterial cellulose in nitrogen atmosphere

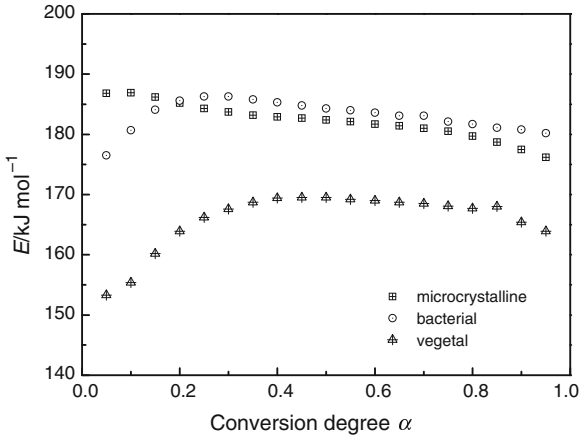

Fig. 5 Distribution of activation energy against conversion degree obtained from Eq. 1 for microcrystalline, bacterial, and vegetal cellulose

The estimated activation energy E, and B, depending on the degree of conversion α, are show in Table 2 and Fig. 5. The largest variation in the activation energy, at approximately 25% conversion, can be attributed to pyrolysis of the amorphous region of the cellulose, which stabilizes when the crystalline region begins to decompose. This behavior is not observed for MCC, probably because the acid treatment primarily affects the amorphous region. The lower activation energy observed for VC may be due to the presence of impurities such as hemicelluloses and lignin, which may vary from 2–4%.

Continuing from experimental curves α–T, the term dα/dT could be determined by numerical integration. Thus, the dα/dT data plus the activation energy from Table 2 could be substituted in the right side of Eq. 3 to obtain the experimental $f(\alpha)g(\alpha)$ for each heating rate against

Table 2 Parameters activation energy and B term obtained from evaluation of the TG data using Eq. 1 and the pre-exponential factor calculated from Eq. 5

Conversion degree, α	Microcrystalline			Bacterial			Vegetal		
	E/kJ/mol	B	ln A 1/min	E/kJ/mol	B	ln A 1/min	E/kJ/mol	B	ln A 1/min
0.05	186.8	42.17	33.95	176.5	39.36	31.11	153.3	34.95	26.71
0.1	186.9	41.81	34.31	180.7	39.64	32.12	155.4	34.86	27.34
0.15	186.2	41.4	34.34	184.1	39.99	32.89	160.2	35.54	28.46
0.2	185.2	41.02	34.27	185.6	40.07	33.29	163.9	36.07	29.3
0.25	184.3	40.7	34.21	186.3	40.05	33.52	166.2	36.37	29.86
0.3	183.7	40.43	34.15	186.3	39.9	33.58	167.6	36.5	30.2
0.35	183.2	40.23	34.14	185.8	39.68	33.55	168.7	36.6	30.49
0.4	182.9	40.06	34.14	185.3	39.48	33.52	169.4	36.62	30.68
0.45	182.7	39.91	34.15	184.8	39.28	33.48	169.5	36.54	30.76
0.5	182.4	39.77	34.16	184.3	39.1	33.45	169.5	36.44	30.81
0.55	182.1	39.61	34.14	184	38.96	33.45	169.2	36.31	30.82
0.6	181.7	39.45	34.11	183.6	38.79	33.42	169	36.18	30.83
0.65	181.4	39.31	34.11	183.1	38.62	33.38	168.7	36.04	30.82
0.7	181	39.14	34.08	183.1	38.54	33.44	168.5	35.91	30.83
0.75	180.5	38.94	34.02	182.1	38.25	33.29	168.1	35.74	30.8
0.8	179.7	38.68	33.91	181.7	38.08	33.27	167.7	35.53	30.74
0.85	178.7	38.38	33.77	181.1	37.77	33.13	168	35.55	30.92
0.9	177.5	38.01	33.59	180.8	37.7	33.25	165.4	34.93	30.49
0.95	176.2	37.58	33.43	180.2	37.43	33.24	163.9	34.52	30.35

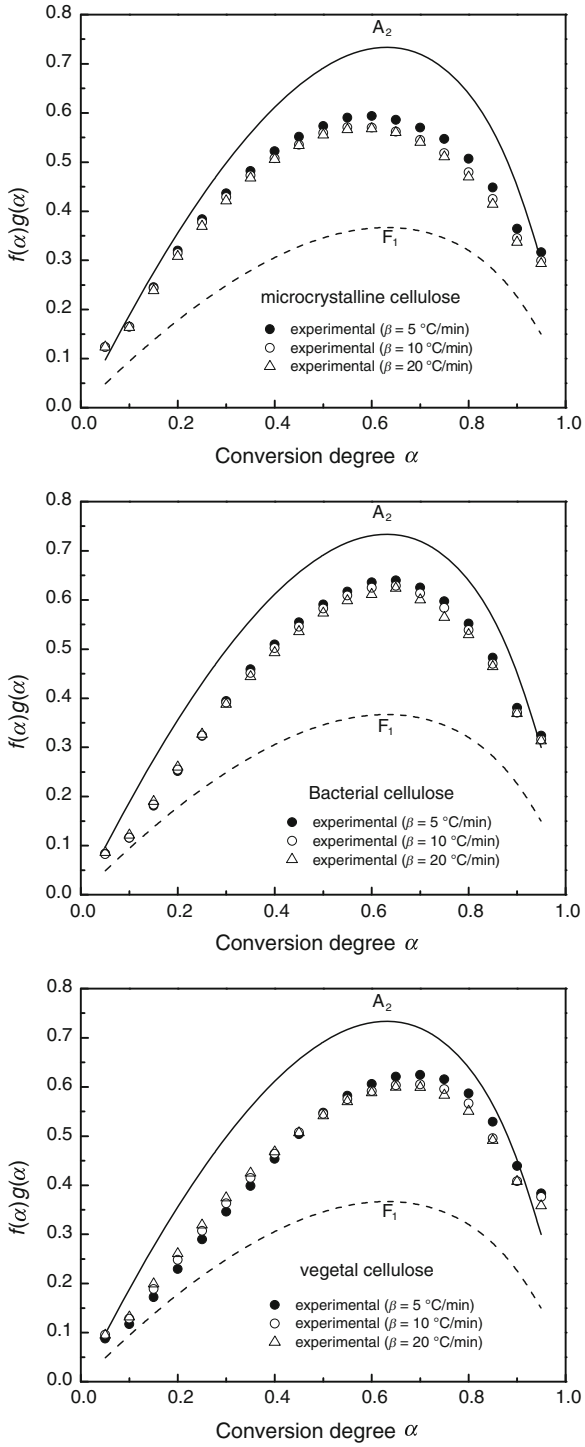

Fig. 6 Theoretical and experimental master plots of $f(\alpha)g(\alpha)$ against α calculated from Eq. 3 for microcrystalline, bacterial, and vegetal cellulose

α, Fig. 6, and then compared with the model from Fig. 2 and Table 1.

The Fig. 6 shows that the experimental values of $f(\alpha)g(\alpha)$ are between the theoretical curves of the model F_1 and A_2. Thus, it can be concluded that the function for the kinetic model follows $g(\alpha) = [-\ln(1-\alpha)]^{1/n}$ where $1 < n < 2$. The estimates for the kinetic exponent n, can be obtained from Eq. 4 and are shown in Table 3.

Table 3 Kinetic exponent calculated from Eq. 4

Cellulose	Heating rate/ °C/min	Kinetic exponent $n \pm$ SD	Adj. R-Square
Microcrystalline	5	1.65 ± 0.02	0.9617
	10	1.59 ± 0.02	0.95506
	20	1.57 ± 0.02	0.95518
	Mean value	1.60 ± 0.03	
Bacterial	5	1.69 ± 0.02	0.97268
	10	1.66 ± 0.02	0.97648
	20	1.63 ± 0.02	0.97988
	Mean value	1.66 ± 0.03	
Vegetal	5	1.64 ± 0.05	0.89774
	10	1.62 ± 0.04	0.92968
	20	1.62 ± 0.03	0.94907
	Mean value	1.63 ± 0.18	

The mean values found for n were from 1.60 to 1.66, showing that the pyrolysis for all celluloses follows the same kinetic model, Avrami–Erofeev, with differences in activation energy. Now that n (Table 3), and, E and B (Table 2) are known, the pre-exponential factor ln A, can be calculated from Eq. 5, and the results are shown in Table 2.

The value of n obtained from kinetic analysis of the data can be interpreted in terms of the nucleation rate equation. The fractional value of n may be related to diffusion-controlled growth, or may arise from distributions of sizes or shapes of the reactant particles [28].

Conclusions

The pyrolysis of celluloses followed kinetic model $g(\alpha) = [-\ln(1-\alpha)]^{1/1.63}$ on average, characteristic for Avrami–Erofeev with only small differences in activation energy. The fractional value of n may be related to diffusion-controlled growth, or may arise from the distributions of sizes or shapes of the reactant particles. The largest variation in the activation energy for approximately 25% conversion was attributed to pyrolysis of the amorphous region of the cellulose, which stabilizes when the crystalline region begins to decompose. This behavior was not observed for MCC, probably because the acid treatment affected the amorphous region. The lower activation energy for VC was attributed to the presence of impurities such as hemicelluloses and lignin.

Acknowledgements The authors acknowledge the FACTE—Fundação de Apoio à Ciência Tecnologia e Educação for financial support.

References

1. Gardner DJ, Oporto GS, Mills R, Samir MASA. Adhesion and surface issues in cellulose and nanocellulose. J Adhesion Sci Technol. 2008;22:545–67.
2. Barud HS, Ribeiro CA, Crespi MS, Martines MA, Dexpert-Ghys J, Marques RFC, Messaddeq Y, Ribeiro SJ L. Thermal characterization of bacterial cellulose–phosphate composite membranes. J Therm Anal Calorim. 2007;87:815–8.
3. Klemm D, Schumann D, Kramer F, Hessler N, Hornung M, Schmauder HP, Marsch S. Nanocelluloses as innovative polymers in research and application. Adv Polym Sci. 2006;205:49–96.
4. Kennedy JF, Phillips GO, Wedlock DJ, Williams PA. Cellulose and its derivatives. Chemistry, biochemistry and applications. UK: Ellis Horwood; 1985.
5. Sjostroom E. Wood chemistry: fundamentals and applications. New York: Academic Press; 1981.
6. Iguchi M, Yamanaka S, Budhiono A. Bacterial cellulose—a masterpiece of nature's arts. J Mater Sci. 2000;35:261–70.
7. Moon RJ. Nanomaterials in the forest products industry. Mcgraw-Hill Yearbook of Science & Technology. New York: McGraw-Hill; 2008.
8. Klemm D, Heublein B, Fink HP, Bohn A. Cellulose: fascinating biopolymer and sustainable raw material. Angew Chem Int Ed. 2005;44:3358–93.
9. Klemm D, Schumann D, Udhardt U, Marsch S. Bacterial synthesized cellulose—artificial blood vessels for microsurgery. Prog Polymer Sci. 2001;26:1561–603.
10. Barud HS, Barrios C, Regiani T, Marques RFC, Verelst M, Ghys JD, Messaddeq Y, Ribeiro SJL. Self-supported silver nanoparticles containing bacterial cellulose membranes. Mat Sci Eng. 2008;C28:515–8.
11. Barud HS, Assunção RMN, Martines MAU, Ghys JD, Marques RFC, Messaddeq Ribeiro Y, Ribeiro SJL. Bacterial cellulose–silica organic–inorganic hybrids. J Sol Gel Sci Technol. 2008;46:363–7.
12. Grande CJ, Torres FG, Gomez CM, Troncoso OP, Canet-Ferrer J, Martínez-Pastor J. Development of self-assembled bacterial cellulose–starch nanocomposites. Mat Sci Eng C. 2009;29:1098–104.
13. Wang J, Gao C, Zhang Y, Wan Y. Preparation and in vitro characterization of BC/PVA hydrogel composite for its potential use as artificial cornea biomaterial. Mater Sci Eng C. 2010;30:214–8.
14. Kramer F, Klemm D, Schumann D, Hessler N, Wesarg F, Fried W, Stadermann D. Nanocellulose polymer composites as innovative pool for (Bio) material development. Macromol Symp. 2006;244:136–48.
15. Hirata T. Changes in degree of polymerization and weight of cellulose untreated with inorganic salts during pyrolysis. For For Prod Res Inst Bull. 1979;304:77–124.
16. YuI Rubtsov, Kazakov AI. Kinetics of heat release during decomposition of cellulose. Combust Explos Shock Waves. 1993;29:710–3.
17. Varhegyi G, Antal MJ Jr. Kinetics of the thermal decomposition of cellulose, hemicellulose, and sugar cane bagasse. Energy Fuels. 1989;3:329–35.
18. Vovelle C, Mellottée H, Delbourgo R. Kinetics of the thermal degradation of cellulose and wood in inert and oxidative atmospheres. Symposium (International) on Combustion. 1982;19:797–805.
19. Akira K. A study on the carbonization process of wood. For For Prod Res Inst Bull. 1979;304:7–76.
20. Bigger SW, Scheirs J, Camino G. An investigation of the kinetics of cellulose degradation under non-isothermal conditions. Polym Degrad Stab. 1998;62:33–40.
21. Emsley AM, Heywood RJ, Ali M, Eley CM. On the kinetics of degradation of cellulose. Cellulose. 1997;4:1–5.
22. Fairbridge C, Ross RA, Sood SP. A kinetic and surface study of the thermal decomposition of cellulose powder in inert and oxidizing atmospheres. J Appl Polym Sci. 1997;22:497–510.
23. Dahiya JB, Kumar K, Muller-Hagedorn M, Bockhorn H. Kinetics of isothermal and non-isothermal degradation of cellulose: model-based and model-free methods. Polym Int. 2008;57:722–9.
24. Capela JMV, Capela MV, Ribeiro CA. Rational approximations of the Arrhenius integral using Jacobi fractions and gaussian quadrature. J Math Chem. 2009;45:769–75.
25. ABNT—Associação Brasileira de Normas Técnicas—NBR 7730.
26. Oliveira RL, Oliveira GC, Meireles CS, de Assunção RMN, Barud HS, Rodrigues Filho G, Messaddeq Y, Ribeiro SJL. Synthesis and characterization of microcrystalline cellulose produced from bacterial cellulose. J Therm Anal Calorim. 2010; submitted.
27. Bolhuis GH, Chawhan ZT. Materials for direct compaction. In: Nyström C, Alderbon G, editors. Pharmaceutical powder compaction technology. New York: Marcel Dekker; 1996.
28. Gawey AK, Brown ME. Thermal decomposition of ionic solids. Amsterdam: Elsevier; 1999.